Desalination and Water Treatment
www.deswater.com

doi: 10.5004/dwt.2020.26000

197 (2020) 328–334
September

Preparation of nanoscale zero-valent metal for catalyzed clean oxidation of hydroxypropyl guar gum at a wide pH range

Ying Tang[a,b,*], Ling Zhou[a], Yuying Xue[a], Xuefan Gu[a,b], Jie Zhang[a], Chengtun Qu[a,c,*]

[a]*College of Chemistry and Chemical Engineering, Xi'an Shiyou University, Xi'an 710065, China, emails: tangying78@xsyu.edu.cn (Y. Tang), xianquct@xsyu.edu.cn (C. Qu), 2081617535@qq.com (L. Zhou), 958362272@qq.com (Y. Xue), xuefangu@xsyu.edu.cn (X. Gu), zhangjie@xsyu.edu.cn (J. Zhang)*
[b]*Shaanxi Key Laboratory of Environmental Pollution Control and Reservoir Protection in Oil and Gas Field, Xi'an 710065, China*
[c]*State Key Laboratory of Petroleum Pollution Control, CNPC Research Institute of Safety and Environmental Technology, Beijing 102206, China*

Received 27 October 2019; Accepted 16 April 2020

ABSTRACT

Metal-persulfate is currently used for $SO_4^{\bullet-}$ generation and oxidation to remove organic contaminants. However, homogeneous metal-persulfate requires acidic pH conditions and metal ions cannot be separated from the bulk after the reaction. To address these issues, a heterogeneous nanoscale zero-valent metal catalyst was used to activate peroxymonosulphate for advanced oxidation of hydroxypropyl guar gum (HPG) and other polymers in oilfield wastewater. It was found that the nanoscale Cu(0) performed high catalytic activity in a wide pH range of 7.0–11.0. The viscosity of HPG can be reduced effectively from 24 to 2.5 with the 10.0% $Na_2S_2O_8$ (mass ratio to HPG) and 10.0% Cu(0) (mass ratio to $Na_2S_2O_8$), and the chemical oxygen demand of HPG solution can be decreased from 7,602 to 1,070 mg L^{-1} in presence of the nanoscale Cu(0). Furtherly, the morphology and pore structure of catalysts were characterized in detail by scanning electron microscopy, X-ray diffraction and Brunauer–Emmett–Teller.

Keywords: Metal-persulfate; Advanced oxidation; Catalytic; Hydroxypropyl guar gum; Oilfield

1. Introduction

Guar gum is a galactomannan extracted from the seeds of *Cyamopsis tetragonoloba*, a native plant of India [1]. It is a non-ionic, water-soluble and because of its low cost and excellent viscoelastic properties, it and its derivatives are extensively used in industrial applications including food, oil recovery, personal care, etc. Structurally it has a biodegradable and biocompatible heteropolysaccharide composed of a β-(1–4) D-mannopyranose backbone linked with α-(1–6) D-galactopyranose units [2–5]. It is one of the most powerful water binder and viscosity enhancer, superior to practically all known water-soluble gums. The main important industrial use of guar gum is as a hydraulic fracturing fluid additive in oil and gas recovery. Now, a guar gum derivative containing hydroxyl group, hydroxypropyl guar gum (HPG), has been widely used as an oilfield fracturing additive because of its high viscosity of aqueous solutions even at low concentrations [6–8]. Therefore, there is a large amount of HPG in the produced water after fracturing which needs to be treated due to its high viscosity, serious corrosion to facilities and potential risks to the health of the residents around the oilfield. So far, the treatment technologies of wastewater containing HPG in China and abroad include advanced oxidation, settlement, neutralization, activated carbon adsorption, ultrafiltration alone or their combination. However, these treatment ways still have some disadvantages such as high operating cost, limited optimum pH range, massive sludge produced and

* Corresponding authors.

so on. Hence, it is urgent to develop effective methods to remove HPG from the contaminated environment.

Hydroxyl radical ($HO^{\bullet}$), as one of the most effective oxidants, generated from the Fenton or Fenton-like process, the supreme oxidation potential of $HO^{\bullet}$ makes it a strong oxidant for water treatment, soil remediation, biological sensors, and material synthesis. However, several drawbacks of the current Fenton process limited their practical applications such as requiring an acidic pH condition and also leading to massive sludge production [9,10]. At high pH values, where the efficiency of the Fenton reagent was diminished, the reactivity of the metal-persulfate was still stable [11,12]. Considering the more active of sulfate radicals ($SO_4^{\bullet-}$) for oxidation with the higher reduction potential of 2.5–3.1 V compared to $HO^{\bullet}$ (1.8–2.7 V) [13,14], metal-persulfate has been studied recently as an oxidant alternative for treating organic contaminants in contaminated produced water in the oilfield with high pH value [15]. However, few researches have been reported to explore persulfate processes catalyzed by zero-valent metal for the effective abatement of polymers such as HPG under an acceptable level.

In this work, the main attempt was devoted to partially destroy HPG contained in oilfield produced water and improve the degradability of the wastewater through the oxidation of metal-persulfate in a wide pH range. The catalyst was screened by the viscosity reduction of the HPG solution oxidized by $Na_2S_2O_8$. The morphology and pore property of the prepared nanoscale zero-valent metal catalyst was thoroughly characterized by various techniques.

2. Experimental procedure

2.1. Materials

All of the reagents were of analytical grade and were used without further purification. HPG, carboxymethyl cellulose (CMC) and polyacrylamide (PAM) (purity > 95%) were obtained from Xinhe Environmental Protection Co., (Zhengzhou, China). Bentonite was obtained from Fengyun Chemical Co., Ltd., Xi'an, China.

2.2. Catalyst preparation

A series of nanoscale zero-valent metal was prepared as Shi et al. [16] described. For example, nanoscale zero-valent copper particles were synthesized by adding an aqueous solution of 0.16 M $NaBH_4$ (98%, Sigma-Aldrich Trading Co., Ltd., Shanghai, China) dropwise to a 0.1 M $CuCl_2$ (98%, Sigma-Aldrich Trading Co., Ltd., Shanghai, China) solution at ambient temperature with magnetic stirring. The freshly synthesized Cu(0) particles were washed with absolute ethyl alcohol three times and then dried in a drying oven at 50°C for use. The zero-valent copper particles produced in this way were characterized by single-point nitrogen adsorption Brunauer–Emmett–Teller (BET) analysis to evaluate the surface area and the size of individual particles ranged [17].

2.3. Experimental procedure

First, 1.2 g guar gum powder was dissolved in 200 ml distilled water at room temperature and stirred for 4 h to form the glue solution. Subsequently, different amounts of $Na_2S_2O_8$ (persulfate, PS) and catalysts were added to the solution weighing to obtain a homogeneous mixture [18]. NaOH was used to adjust the pH value [19]. Finally, the obtained mixture was poured into an Ubbelohde viscometer at a certain temperature and then measured the viscosity intermittently and relative molecular mass. The $Na_2S_2O_8$ concentration, catalyst amount, reaction temperature and pH were investigated in detail because of their significant effects on the oxidation capacity. The chemical oxygen demand (COD) was determined according to the standard dichromate method according to the GB11914 of China and ISO6060.

2.4. Characterization of catalysts

The morphology of the prepared catalysts was elucidated using a scanning electron microscope (SEM, JSM-6390A, JEOL, Japan) with 20.0 kV of an accelerating voltage. Surface area and pore property measurements were performed by N_2 physisorption using a Micromeritics ASAP 2020 HDBB instrument (Norcross, GA, USA) at 77 K. The surface areas were calculated using the BET equation in the pressure of range P/P^0 = 0.02–0.2, and the pore size distribution was calculated using the Barrett–Joyner–Halenda method. The phase structures of the calcinated catalysts were analyzed using an X-ray diffraction (XRD) device (JDX-3530, JEOL, Japan) with an X-ray tube having copper (Cu) as a target and released Kα radiation when accelerated at 40 mA and 40 kV, arranged at 5°–80° with a scanning speed of 2 min^{-1}. Morphologies of the Cu(0) nanocatalyst before and after reactions were characterized by scanning electron microscopy (SEM), X-ray and BET.

3. Results and discussion

3.1. Catalytic performance

3.1.1. Screening of catalysts

As we have known that persulfate can be activated to produce $SO_4^{\bullet-}$ by using transition metals as a catalyst [20]. The catalytic performance of each zero-valent metal in the presence of $Na_2S_2O_8$ to degrade hydroxypropyl guar can be reflected by the relative viscosity of it due to small molecular will produce after hydroxypropyl guar degradation, which caused the viscosity of the solution decrease because the viscosity of the solution greatly depended on the extent of hydroxypropyl guar degradation. The degradation performance of HPG solution with the mass concentration of 0.6% was investigated under 10% $Na_2S_2O_8$ (mass ratio to HPG), 45°C, pH 7.0 over various 10% zero-valent metal catalyst (mass ratio to $Na_2S_2O_8$) of Cr(0), Mn(0), Fe(0), Co(0), Ni(0), Cu(0) and Zn(0). The results are summarized in Fig. 1. From the results, it can be seen that all of the zero-valent metal show their catalytic performance to degrade HPG in the presence of $Na_2S_2O_8$, and the relative viscosity of HPG solution was decreased greatly at the initial reaction time of 10 min. However, further extension of reaction time plays no more efficiency on the degradation and the relative viscosity of HPG solution showed a great decrease from 24 to 2.5 in presence of Cu(0)

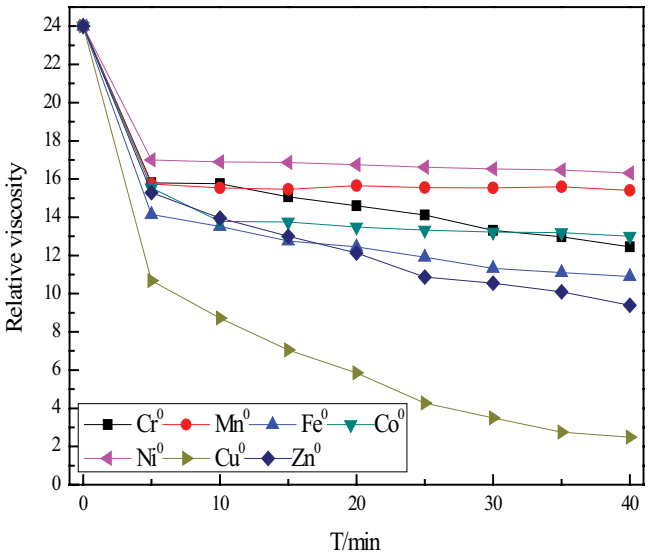

Fig. 1. Degradation performance over different zero-valent metal catalysts.

during the reaction time. If Cu^{2+} was chosen as a catalyst for active PS, it should control the pH of the wastewater in a low value to avoid the deposition of the metal ions.

The reaction and catalytic process of the Cu-PS system were described as the following equations [21]. Some intrinsic drawbacks of the Cu^{2+}-PS system may restrict its practical application. Reactions involving in the Cu^{2+}-PS process are illustrated in Eqs. (1) and (2). In addition, $SO_4^{\bullet-}$ can be consumed by reacting with excessive Cu^{2+} in the solution [Eq. (2)], which results in reduced degradation efficiency of target contaminants.

$$S_2O_8^{2-} + Cu^{2+} \rightarrow Cu^{3+} + SO_4^{\bullet-} + SO_4^{2-} \quad (1)$$

$$SO_4^{\bullet-} + Cu^{2+} \rightarrow Cu^{3+} + SO_4^{2-} \quad (2)$$

$$Cu^0 + H_2O + 0.5O_2 \rightarrow Cu^{2+} + 2OH^- \text{ (oxic conditions)} \quad (3)$$

$$Cu^0 + 2H_2O \rightarrow Cu^{2+} + 2OH^- + H_2 \text{ (anoxic conditions)} \quad (4)$$

$$S_2O_8^{2-} + Cu^0 \rightarrow Cu^{2+} + 2SO_4^{2-} \quad (5)$$

$$Cu^0 + 2Cu^{3+} \rightarrow Cu^{2+} \quad (6)$$

Zero-copper iron can serve as an alternative source of Cu^{2+}. In Cu(0)-PS system, Cu^{2+} is produced by zero-valent copper corrosion under oxic/anoxic condition and/or oxidation by PS [Eqs. (3)–(5)]. Unlike homogeneous Cu^{2+} activation, Cu^{2+} has gradually released into the aqueous solution in the Cu(0)-PS system. In this way, accumulation of excessive Cu^{2+} and the subsequent quenching of $SO_4^{\bullet-}$ (Eq. (2)) can be largely minimized. In addition, Cu^{2+} can be regenerated by recycling Cu^{3+} at the surface of zero-valent copper through Eq. (6). Thus, the utilization efficiency of PS is greatly improved [22–25]. These advantages of Cu(0)-PS process have been well demonstrated in previous studies and Cu(0) is illustrated more stable as a result the generated sulfate radicals may be mainly consumed by HPG oxidation. Another potential mechanism of enhanced HPG oxidation may be the generation of Cu^{3+}, which is unstable and may act as an oxidant for HPG degradation. The recurred Cu^{2+} in this process was capable of activating persulfate, which may explain the well-maintained HPG degradation efficiency throughout the entire reaction [26,27].

3.1.2. Effect of dosage of catalyst

To optimize the catalytic performance of Cu(0), the dosage of catalyst in the reaction was investigated in the following work. Fig. 2 shows the results of the relative viscosity of HPG oxidized by $Na_2S_2O_8$ at various dosages of catalyst ranged from 1% to 15% (molar ratio to $Na_2S_2O_8$) at 45°C and pH 7.0. As we can see, Cu(0) dosage has a significant effect on the degradation of guar gum. The decrease of relative viscosity of HPG improved significantly with increasing catalyst dosage from 1% to 10%. Above 10%, since the reactive sites were enough, no further increase of the HPG degradation can be obtained, which should be due to the consumption of generated $SO_4^{\bullet-}$ by the excess catalyst as suggested by Wang et al. [28]. Thus, 10% was chosen as the optimum dosage in the following experiments.

3.1.3. Effect of temperature

The temperature plays an important role in chemical oxidation because it represents a determinant reaction rate and heat [29]. The effect of reaction temperature was evaluated on the degradation of HPG at 25°C, 30°C, 35°C, 40°C, and 45°C using Cu(0) as the catalyst at pH 7.0. Fig. 3 demonstrates the variation of viscosity of HPG solution at various reaction temperatures in the presence of 10% $Na_2S_2O_8$. As shown, the relative viscosity of the HPG solution decreased significantly with the increase of reaction temperature, and the best performance was obtained under 45°C. It is consistent with the result that the oxidation degradation is an endothermal reaction, and the higher reaction temperature is good to the degradation process [30]. Based on the application condition in the oilfield, the temperature was not screened further.

3.1.4. Effect of pH

The pH effect on the oxidation degradation process was studied in the previous studies to be quite significant by mainly affecting the species distributions of Cu and sulfate and consequently tuned the Cu(0)-PS reaction by causing the hydration of Cu to produce Cu–OH complex species as suggested by Chen et al. [31]. At neutral and acidic solution, a hydrated shell around Cu–OH complex can be formed, thus impeding the direct contact between the inner core of Cu–OH complexes and the sulfate. At higher pH, the fraction of protonated complexes decreases, whereas that of deprotonated complexes increases, leading to the facilitated reaction between the catalytic active inner core of Cu and sulfate anion. Therefore, higher pH leads to a more efficient generation of $SO_4^{\bullet-}$ in the Cu-PS reaction system, resulting in higher efficient degradation performance.

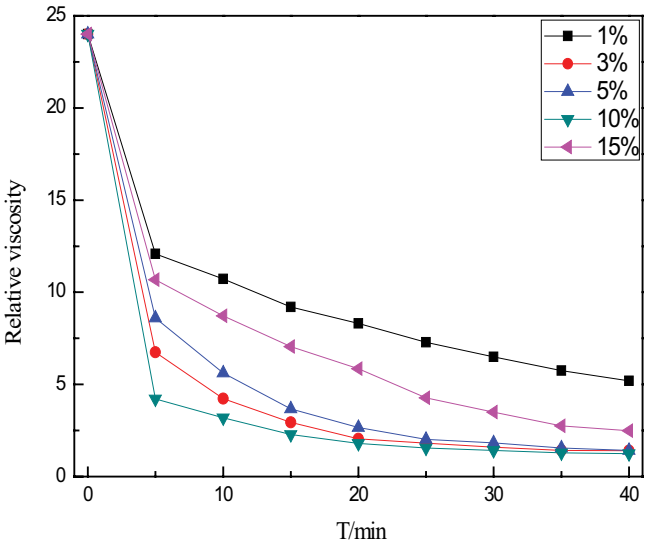

Fig. 2. Effect of Cu(0) dosage on hydroxypropyl guar gum degradation.

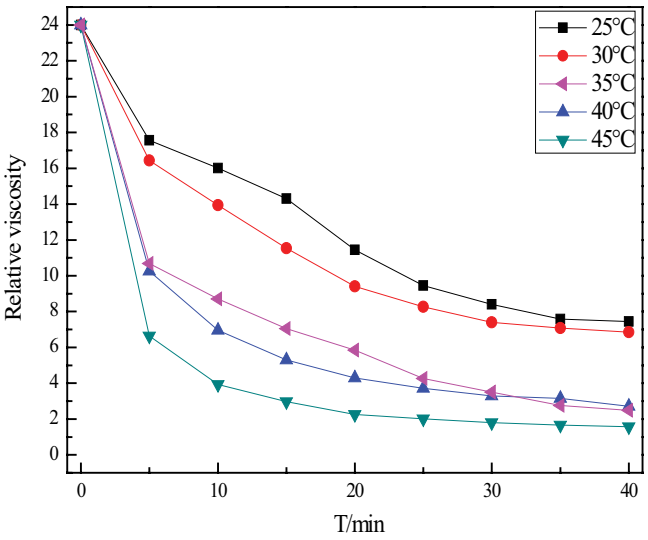

Fig. 3. Effect of reaction temperature on hydroxypropyl guar gum degradation.

In our research, the degradation of HPG was examined at pH range from 7 to 11 with the HPG concentration of 0.6% at 45°C, and the results are summarized in Fig. 4. In order to well illustrate the effect of pH on the degradation of HPG, the relative viscosity at initial reaction time was recorded at 5 min. From the result, it can be found that the obvious decrease of the relative viscosity of HPG from 5 to 1.25 can be obtained, even the oxidation degradation was conducted under high pH conditions of 11, indicating that the generation of reactive oxygen species by the zero-valent metal copper is pH-dependent, which influences the dissolution and existential state of metal ion so as to the evolution of the superoxide radical.

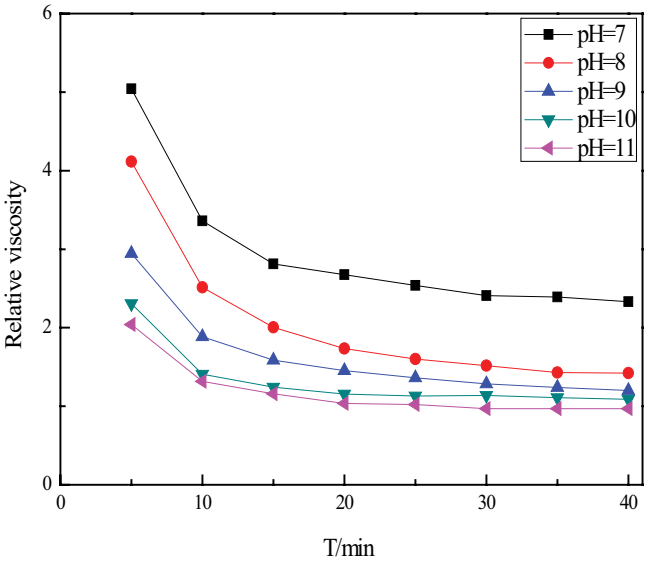

Fig. 4. Effect of pH on hydroxypropyl guar gum degradation.

3.1.5. COD removal

To determine the extent of degradation, the relative molecular weight of HPG after oxidation catalyzed by Cu(0) in presence of 10% $Na_2S_2O_8$ was determined by specific viscosity (ηsp) and the relative viscosity (ηr) over a series of different HPG concentrations measured at 45°C and pH 9 using Ubbelohde viscometer according to the method reported by Netopilík et al [32]. Reduced values of both ηsp and ηr were extrapolated to zero to obtain the intrinsic viscosity [33]. As shown in Fig. 5, the intrinsic viscosity was close to 0.12 and the average molecular weight of HPG can be dropped to 2,947 from 2 million after oxidation treatment. Furthermore, the specific viscosities measured at 45°C showed a great dependence on polymer concentration which was probably due to values of ηsp/c at low concentrations affected by adsorption of the capillary wall [34].

To ascertain COD removal efficiency in oilfield wastewater which containing HPG, PAM and CMC, degradations of the three polymers were conducted by Cu(0)-PS and the results are presented in Fig. 6. The three polymers with the mass concentration of 0.6% were oxidized by 100% $Na_2S_2O_8$ (the demand of $Na_2S_2O_8$ to oxidize the polymer to CO_2 and H_2O) at 45°C and pH 10 respectively. From Fig. 6 it can be seen that Cu(0) has great catalytic degradation performance to various polymers and the COD removal efficiency of HPG, PAM and CMC was 59.9%, 46.3% and 55.6% within 45 min, respectively, and after 240 min at same conditions, the COD removal efficiency enhanced to 85.9%, 82.1% and 85.1%. Moreover, the COD removal efficiency for HPG was equal to the treatment efficiency by coagulation and the UV/H_2O_2/ferrioxalate complexes process that overall removal efficiency of COD reached 83.8% at pH of 4 and $FeCl_3$ loading of 1,000 mg L^{-1} in the coagulation process [35]. It also can be found that HPG is easier to be oxidized than others due to its natural linear galactomannan gum consisting of a linear backbone of β-1,4 linked mannose units and randomly attached α-1,6 linked galactose

units as side chains [36] which is more easily degraded than the other two polymers for the easy decomposition characteristics of side-chain galactose as suggested in Fig. 7.

3.2. Catalyst characterization

To investigate the stability of the catalyst, it is important to clarify the structure of the catalyst before and after the reaction process. Fig. 8 depicts the SEM images of the surface morphology of Cu(0) after the catalyst had been recycled five times at 5000 times magnification before (Fig. 8a) and after (Fig. 8b) degradation. It can be seen that the particle size and surface morphology of the used Cu(0) are different from the newly prepared Cu(0). The surface of the catalyst before reaction mainly appears in the flake particles state with smaller particle size, while the particle size of the catalyst was relatively larger and appeared as aggregate flake particles after recycling reaction, indicating its decreasing of surface area so as to its catalytic activity.

BET gas absorptiometry measurements were conducted to examine the porous nature of the Cu(0) catalyst. Fig. 9 illustrates the N_2 adsorption-desorption isotherms. From the result, it can be seen the accretion of nitrogen adsorption accompanied by hysteresis of both Cu(0) samples belongs to type IV with the high relative pressure, which is characteristic of mesoporous materials [37]. From Table 1, the BET specific surface area of the fresh Cu(0) calculated from N_2 isotherms at –196.6°C was found to be as much as 15.8798 $m^2 g^{-1}$ with a pore volume of 0.0373 $cm^{-3} g^{-1}$. Furthermore, the BET specific surface area of Cu(0) after the catalyst had been recycled for five times was found to be as much as 14.219 $m^2 g^{-1}$ with a pore volume of 0.0195 $cm^{-3} g^{-1}$. It can be concluded that the decrease of the BET area, pore size and pores volume of reclaimed Cu(0) with the reusability time caused the decrease of catalytic performance over reused catalyst. The destroy of catalyst structure after degradation can be further confirmed according to the results of the microstructures of reusable catalysts as shown in Fig. 8b that the good dispersion of fresh Cu(0) catalyst became to exhibits agglomeration to some extent with reused time [38].

The XRD patterns of zero-valent copper before and after degradation are presented in Fig. 10. From the results, it can be seen that the components of the catalysts mainly include Cu(0) (2θ = 43.26° and 50.04°) [39] and NaCl (2θ = 28.64°, 31.77°, 47.16°, 56.58°, and 66.28°) (JCPDS 4–836) crystal phases. The diffraction peak of Cu(0) at 43.3° is sharp and intense indicating their highly crystalline nature. Moreover, the XRD pattern is essentially identical to that of the simulated XRD pattern of Cu(0) powder, verifying the successful synthesis of Cu(0). The most common (100) crystal phases were found at 31.77° assigned to NaCl [40] due to the catalyst preparation process carried out by $NaBH_4$ reduction of $CuCl_2$ to prepare zero-valent copper. NaCl was formed as the by-product. Furthermore, the surface of

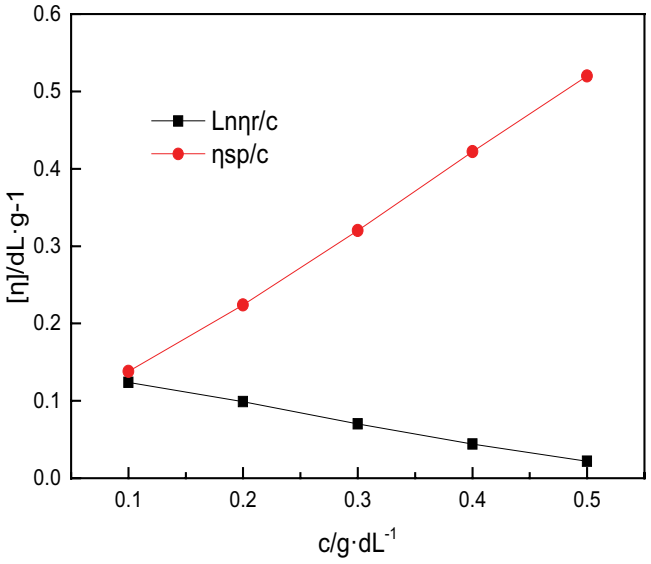

Fig. 5. ηsp/c-c and lnηr/c-c.

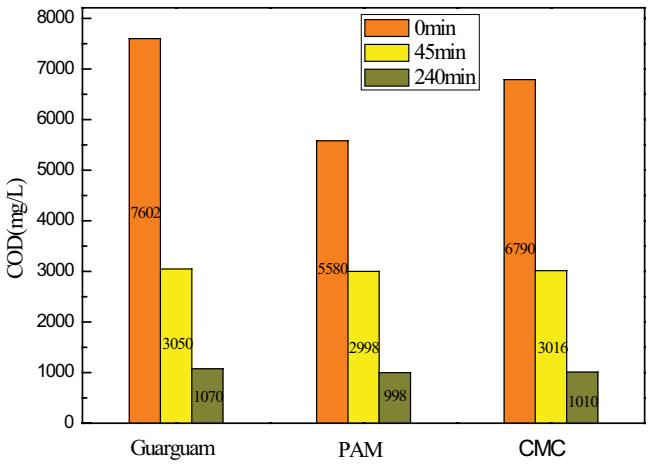

Fig. 6. COD removal over Cu(0) on three different polymers.

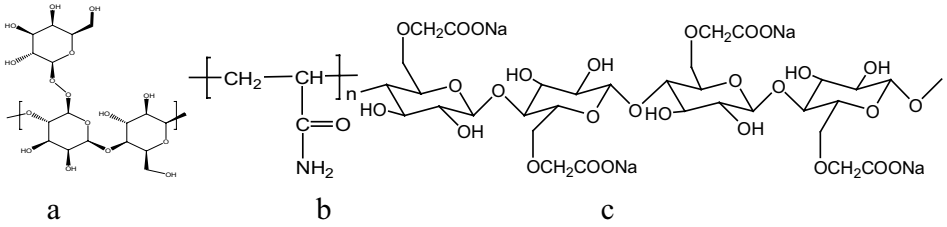

Fig. 7. Structure of guar gum (a), PAM (b), and CMC (c).

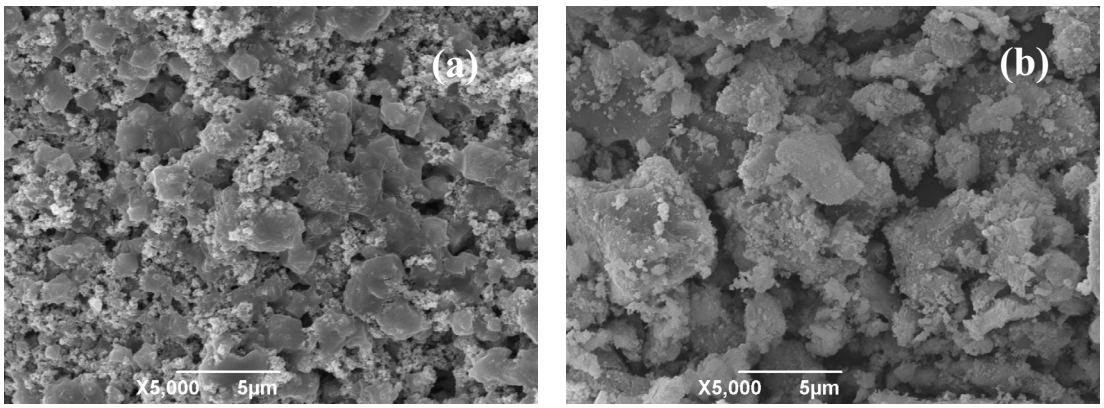

Fig. 8. SEM images of the reclaimed Cu(0) catalyst (a) reclaimed 0 and (b) reclaimed 5.

Table 1
Pore properties of Cu(0) before and after degradation

Catalyst	Pore size (nm)	Pore volume ($cm^3 g^{-1}$)	Surface area ($cm^2 g^{-1}$)
Cu(0)(before)	9.4062	0.037342	15.8798
Cu(0)(after)	3.8548	0.019485	4.2190

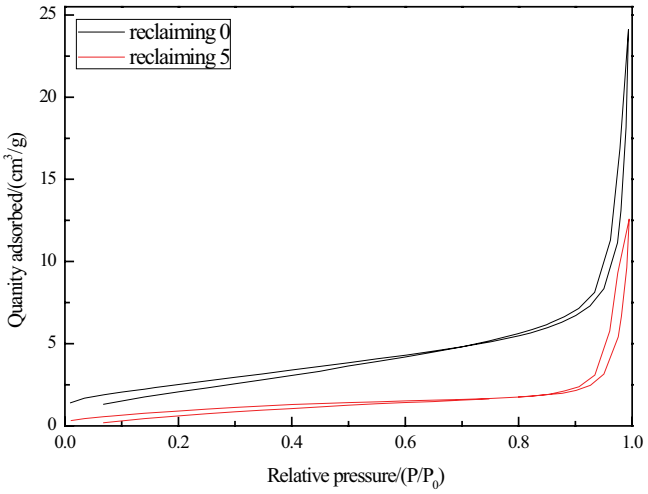

Fig. 9. N_2 adsorption/desorption isotherms of Cu(0) before and after degradation.

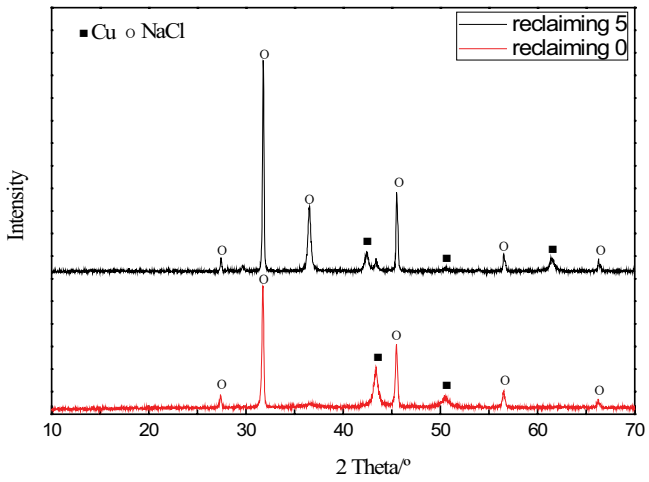

Fig. 10. XRD patterns of Cu(0) before and after degradation.

the synthesized zero-valent metal copper catalyst is assembled from nanosized particles, which is in good accordance with the SEM results.

4. Conclusions

A series of nanoscale zero-valent metal catalysts was prepared to be used as the oxidation catalysts under a wide pH range. The catalyst was screened by the relative viscosity reduction of HPG solution oxidized by $Na_2S_2O_8$, and Cu(0) exhibited the highest catalytic performance for the degradation of HPG in a wide pH range of 7.0–11.0, and the relative viscosity of HPG can be reduced effectively with the 10.0% $Na_2S_2O_8$ (mass ratio to HPG) and 10.0% Cu(0) (mass ratio to $Na_2S_2O_8$). Moreover, the high degradation efficiency over prepared Cu(0) even can be obtained for various polymers commonly used in the oilfield at high pH value up to 10 with enough $Na_2S_2O_8$ within 4 h. The results offer an attractive alternative way in disposing of the recalcitrant fracturing wastewater.

Acknowledgments

The work was supported financially by National Science Foundation of China (No. 21763030), Scientific Research Plan Projects of Shaanxi Science and Technology Department (2019GY-136) and Xi'an Science and Technology Project (201805038YD16CG22(3)), Postgraduate Innovation and Practical Ability Training Project of Xi'an Shiyou University

(YCS18211017). And we thanks the work of Modern Analysis and Testing Center of Xi'an Shiyou University.

References

[1] R. Lapasin, L. De Lorenzi, S. Pricl, G. Torriano, Flow properties of hydroxypropyl guar gum and its long-chain hydrophobic derivatives, Carbohydr. Polym., 28 (1995) 195–202.

[2] J. Reuben, Description of heteropolysaccharide ethers: hydroxypropyl guar and carboxymethyl guar, Macromolecules, 18 (1985) 2035–2037.

[3] T.T. Reddy, S. Tammishetti, Free radical degradation of guar gum, Polym. Degrad. Stab., 86 (2004) 455–459.

[4] L.R.S. Moreira, E.X.F. Filho, An overview of mannan structure and mannan-degrading enzyme systems, Appl. Microbiol. Biotechnol., 79 (2008) 165.

[5] Y.C. Zhao, J.P. He, X.X. Han, X.L. Tian, M.Y. Deng, W.P. Chen, B. Jiang, Modification of hydroxypropyl guar gum with ethanolamine, Carbohydr. Polym., 90 (2012) 988–992.

[6] K. Yu, D. Wong, J. Parasrampuria, D. Friend, Guar gum, Anal. Profiles Drug Subst. Excipients, 24 (1996) 243–276.

[7] J.J. Patel, M. Karve, N.K. Patel, Guar gum: a versatile material for pharmaceutical industries, Int. J. Pharm. Pharm. Sci., 6 (2014) 13–19.

[8] N. Thombare, U. Jha, S. Mishra, M.Z. Siddiqui, Guar gum as a promising starting material for diverse applications: a review, Int. J. Biol. Macromol., 88 (2016) 361–372.

[9] S. Enami, Y. Sakamoto, A.J. Colussi, Fenton chemistry at aqueous interfaces, Proc. Natl. Acad. Sci. U.S.A., 111 (2014) 623–628.

[10] X.-J. Yang, X.-M. Xu, J. Xu, Y.-F. Han, Iron oxychloride (FeOCL): an efficient fenton-like catalyst for producing hydroxyl radicals in degradation of organic contaminants, J. Am. Chem. Soc., 135 (2013) 16058–16061.

[11] X.Y. Zhang, Y.B. Ding, H.Q. Tang, X.Y. Han, L.H. Zhu, N. Wang, Degradation of bisphenol A by hydrogen peroxide activated with $CuFeO_2$ microparticles as a heterogeneous Fenton-like catalyst: efficiency, stability and mechanism, Chem. Eng. J., 236 (2014) 251–262.

[12] J. Criquet, N.K.V. Leitner, Degradation of acetic acid with sulfate radical generated by persulfate ions photolysis, Chemosphere, 77 (2009) 194–200.

[13] P. Shukla, H.Q. Sun, S.B. Wang, H. Ming Ang, M.O. Tadé, Co-SBA-15 for heterogeneous oxidation of phenol with sulfate radical for wastewater treatment, Catal. Today, 175 (2011) 380–385.

[14] X.N. Li, Z.H. Wang, B. Zhang, A.I. Rykov, M.A. Ahmed, J.H. Wang, $FexCo_{3-x}O_4$ nanocages derived from nanoscale metal-organic frameworks for removal of bisphenol A by activation of peroxymonosulfate, Appl. Catal., B, 181 (2016) 788–799.

[15] A. Rastogi, S.R. Al-Abed, D.D. Dionysiou, Sulfate radical-based ferrous–peroxymonosulfate oxidative system for PCBs degradation in aqueous and sediment systems, Appl. Catal., B, 85 (2009) 171–179.

[16] D. Shi, X. Zhang, J. Wang, J. Fan, Highly reactive and stable nanoscale zero-valent iron prepared within vesicles and its high-performance removal of water pollutants, Appl. Catal., B, 221 (2018) 610–617.

[17] S.H. Joo, A.J. Feitz, T.D. Waite, Oxidative degradation of the carbothioate herbicide, molinate, using nanoscale zero-valent iron, Environ. Sci. Technol., 38 (2004) 2242–2247.

[18] L.Y. Xu, L. Sun, J. Feng, L.L. Qi, I. Muhammad, J. Maher, X.Y. Cheng, W.M. Song, Nanocasting synthesis of an iron nitride-ordered mesopore carbon composite as a novel electrode material for supercapacitors, RSC Adv., 7 (2017) 44619–44625.

[19] S. Bao, S.-H. Luo, S.-X. Yan, Z.-Y. Wang, Q. Wang, J. Feng, Y.-L. Wang, T.-F. Yi, Nano-sized MoO_2 spheres interspersed three-dimensional porous carbon composite as advanced anode for reversible sodium/potassium ion storage, Electrochim. Acta, 307 (2019) 293–301.

[20] M. Zhang, X.Q. Chen, H. Zhou, M. Murugananthan, Y.R. Zhang, Degradation of p-nitrophenol by heat and metal ions co-activated persulfate, Chem. Eng. J., 264 (2015) 39–47.

[21] X.-R. Xu, X.-Z. Li, Degradation of azo dye Orange G in aqueous solutions by persulfate with ferrous ion, Sep. Purif. Technol., 72 (2010) 105–111.

[22] C.J. Liang, M.-C. Lai, Trichloroethylene degradation by zero valent iron activated persulfate oxidation, Environ. Eng. Sci., 25 (2008) 1071–1078.

[23] C.J. Liang, Y.-Y. Guo, Mass transfer and chemical oxidation of naphthalene particles with zerovalent iron activated persulfate, Environ. Sci. Technol., 44 (2010) 8203–8208.

[24] I. Hussain, Y.Q. Zhang, S.B. Huang, X.Z. Du, Degradation of *p*-chloroaniline by persulfate activated with zero-valent iron, Chem. Eng. J., 203 (2012) 269–276.

[25] S.-Y. Oh, S.-G. Kang, P.C. Chiu, Degradation of 2,4-dinitrotoluene by persulfate activated with zero-valent iron, Sci. Total Environ., 408 (2010) 3464–3468.

[26] X.H. Xu, Q.F. Ye, T.M. Tang, D.H. Wang, Hg^0 oxidative absorption by $K_2S_2O_8$ solution catalyzed by Ag^+ and Cu^{2+}, J. Hazard. Mater., 158 (2008) 410–416.

[27] C.S. Liu, K. Shih, C.X. Sun, F. Wang, Oxidative degradation of propachlor by ferrous and copper ion activated persulfate, Sci. Total Environ., 416 (2012) 507–512.

[28] N. Wang, T. Zheng, G.S. Zhang, P. Wang, A review on Fenton-like processes for organic wastewater treatment, J. Environ. Chem. Eng., 4 (2016) 762–787.

[29] S.W. Wang, Z.W. Li, Q.L. Yu, Kinetic degradation of guar gum in oilfield wastewater by photo-Fenton process, Water Sci. Technol., 75 (2016) 11–19.

[30] E.H. Li, X.Y. Jiao, C.G. Wang, Y.H. Wang, W.S. Wang, G. Liu, D.N. Li, X.J. Meng, B. Li, Degradation kinetics and stability of anthocyanins from blueberry, Food Sci., 39 (2018) 1–7.

[31] L. Chen, X.Y. Huang, M. Tang, D. Zhou, F. Wu, Rapid dephosphorylation of glyphosate by Cu-catalyzed sulfite oxidation involving sulfate and hydroxyl radicals, Environ. Chem. Lett., 16 (2018) 1507–1511.

[32] M. Netopilík, M. Bohdanecký, Ubbelohde viscometer modified for foaming solutions of water soluble polymers, Eur. Polym. J., 31 (1995) 289–290.

[33] Y. Tang, H. Ren, P.W. Yang, H. Li, J. Zhang, C.T. Qu, G. Chen, Treatment of fracturing fluid waste by Fenton reaction using transition metal complexes catalyzes oxidation of hydroxypropyl guar gum at high pH, Environ. Chem. Lett., 17 (2019) 559–564.

[34] Y.F. Shen, J. Tang, Z.H. Nie, Y.D. Wang, Y. Ren, L. Zuo, Tailoring size and structural distortion of Fe_3O_4 nanoparticles for the purification of contaminated water, Bioresour. Technol., 100 (2009) 4139–4146.

[35] Y. Cheng, K.M. Brown, R.K. Prud'homme, Characterization and intermolecular interactions of hydroxypropyl guar solutions, Biomacromolecules, 3 (2002) 456–461.

[36] Z.C. Zhang, Combined treatment of hydroxypropyl guar gum in oilfield fracturing wastewater by coagulation and the UV/H_2O_2/ferrioxalate complexes process, Water Sci. Technol., 77 (2018) 565–575.

[37] W. Yang, W. Yang, L. Kong, A.L. Song, X.J. Qin, G.J. Shao, Phosphorus-doped 3D hierarchical porous carbon for high-performance supercapacitors: a balanced strategy for pore structure and chemical composition, Carbon, 127 (2018) 557–567.

[38] Q.H. Du, L. Su, L.Y. Hou, G. Sun, M.Y. Feng, X.C. Yin, Z.P. Ma, G.J. Shao, W.M. Gao, Rationally designed ultrathin Ni-Al layered double hydroxide and graphene heterostructure for high-performance asymmetric supercapacitor, J. Alloys Compd., 740 (2018) 1051–1059.

[39] F. Zhu, L.W. Li, S.Y. Ma, Z.F. Shang, Effect factors, kinetics and thermodynamics of remediation in the chromium contaminated soils by nanoscale zero valent Fe/Cu bimetallic particles, Chem. Eng. J., 302 (2016) 663–669.

[40] C. Rodriguez-Navarro, L. Linares-Fernandez, E. Doehne, E. Sebastian, Effects of ferrocyanide ions on NaCl crystallization in porous stone, J. Cryst. Growth, 243 (2002) 503–516.